Acta Oceanol. Sin., 2014, Vol. 33, No. 11, P. 112–122
DOI: 10.1007/s13131-014-0560-0
http://www.hyxb.org.cn
E-mail: hyxbe@263.net

The observed analysis on the wave spectra of Hurricane Juan (2003)

XU Fumin[1]*, BUI THI Thuy Duyen[1], PERRIE Will[2]
[1] Key Laboratory of Coastal Disaster and Defense, Ministry of Education, College of Harbour, Coastal and Offshore Engineering, Hohai University, Nanjing 210098, China
[2] Fisheries & Oceans Canada, Bedford Institute of Oceanography, Dartmouth B2Y 4A2, Canada

Received 22 April 2013; accepted 11 June 2014

Abstract
Hurricane Juan provides an excellent opportunity to probe into the detailed wave spectral patterns and spectral parameters of a hurricane system, with enough wave spectral observations around Juan's track in the deep ocean and shallow coastal water. In this study, Hurricane Juan and wave observation stations around Juan's track are introduced. Variations of wave composition are discussed and analyzed based on time series of one-dimensional frequency spectra, as well as wave steepness around Juan's track: before, during, and after Juan's passing. Wave spectral involvement is studied based on the observed one-dimensional spectra and two-dimensional spectra during the hurricane. The standardization method of the observed wave spectra during Hurricane Juan is discussed, and the standardized spectra show relatively conservative behavior, in spite of the huge variation in wave spectral energy, spectral peak, and peak frequency during this hurricane. Spectral widths' variation during Hurricane Juan are calculated and analyzed. A two-layer nesting WW3 model simulation is applied to simulate the one-dimensional and two-dimensional wave spectra, in order to examine WW3's ability in simulating detailed wave structure during Hurricane Juan.

Key words: Hurricane Juan, wave spectra, wave steepness, spectral width, WW3

Citation: Xu Fumin, Bui Thi Thuy Duyen, Perrie Will. 2014. The observed analysis on the wave spectra of Hurricane Juan (2003). Acta Oceanologica Sinica, 33(11): 112–122, doi: 10.1007/s13131-014-0560-0

1 Introduction

Harsh ocean environments present risks to human activities and ocean, marine and coastal engineering, in which hurricane-generated waves are the most devastating and primary factor. It is important to consider the statistical and spectral properties of ocean waves, as their seemingly random characteristics strongly affect the reliability and durability of marine structures and ocean shipping. Wave spectra can reveal the detailed inner structure of ocean waves. One of the most outstanding observed wave spectral studies in the past, the PM spectral form (Pierson and Moskowitz, 1964) is designed for fully developed waves. The JONSWAP spectrum (Hasslemann et al., 1973; Battjes et al., 1987) has been applied widely in theoretical studies, targetting spectra for laboratory experiments and operational wave modelling. The TMA spectrum extends the applicability of the JONSWAP spectrum from deep water to arbitrarily deep water, by introducing a simple form of transformation function (Bouws et al., 1985). The FRF spectrum, based on the approximation of f^4 tail (the corresponding wavenumber spectrum in deep water would be proportional to $k^{-5/2}$) is proposed (Miller and Vincent, 1990), and this fits well with observed spectra, later found to be forced by the quadruplet wave-wave interactions in shallow water (Resio et al., 2001). An improved JONSWAP spectral formulation (Goda, 1988) has been developed, to avoid the difficulties in defining the accurate fetch and getting stable sustained local winds in the original JONSWAP form. However, none of the above spectral formulations can ensure a reasonable fit for hurricane-generated wave spectra.

In hurricane-generated waves, strong wind waves and swell coexist, so wave strength and wave direction change dramatically during a hurricane. It is impossible to deploy enough buoys to measure wave spectra in a hurricane area. Up until now, there have never been enough measurements available for a hurricane-generated wave spectral study. Numerical studies have been carried out to simulate hurricane-generated waves, and wave models generally can provide wave parameters, including wave height, wave period, and wave length, with high precision. However, even the most up-to-date spectral wave models are still not able to simulate wave spectral structure accurately, especially for hurricane-generated waves, which include strong wind waves and swell, and which continuously change with time and space. These hurricane-generated wave spectra are usually multi-peak spectra, and therefore their spectral patterns change dramatically during each hurricane. Hurricane Juan (Sep., 2003) was one of the most devastating storms in the history of Nova Scotia, Canada, and there happened to be several buoys located within the area affected by Hurricane Juan: on the hurricane's direct track, to the right and left sides of its track, on the maximum wind radius, in deep open ocean, and in shallow coastal water. Therefore, Hurricane Juan provided us the best opportunity to explore hurricane-generated wave spectral patterns and variation during its course.

Foundation item: The National Natural Science Foundation of China under contract No. 50779015; the National Key Technology R&D Program of China under contract No. 2012BAB03B01.
*Corresponding author, E-mail: xfm67@hotmail.com

2 Hurricane Juan and wave observation stations around Juan's track

2.1 *Hurricane Juan*

Detailed discussion of Hurricane Juan's development is given by Fogarty et al. (2006) and the Canadian Hurricane Center (http://projects.novaweather.net/work.html). Juan reached hurricane strength by 12:00UTC on Sep. 26 2003 near Bermuda, and it moved northward and then northwestward, as a subtropical ridge, to the northeast of its location, extended to the west. It reached a maximum sustained wind intensity of 46.30 m/s at 18:00UTC on Sep. 27, and then turned northward to Nova Scotia, with increasing propagation speed. By 18:00UTC on Sep. 28, Juan was in the north of the Gulf Stream, and its intensity began to weaken due to the cooler shelf waters south of Nova Scotia. Figure 1 shows Hurricane Juan's track and observation stations in the Northwest Atlantic. Figure 2 shows Hurricane Juan's track near the Scotian Shelf. However, Juan spent little time over these cooler waters and therefore did not weaken significantly, because of its accelerating translational speed. Juan made landfall near Halifax (03:00UTC on 29), with sustained winds of 43.72 m/s. Figure 3 is a satellite image when Juan made landfall in Halifax. Figure 4 shows QSCAT winds at 22:12UTC on Sep. 28, 2003, when Hurricane Juan arrived at the Scotian Shelf. Table 1 gives the best track data of Hurricane Juan. Hurricane Juan's wind and waves around its track have been studied in studies by Xu et al. (2007), and numerically simulated wave parameters fit well with observations.

Spectral wave models (WW3 and SWAN) show the ability to provide numerical simulated wave spectral general properties during a hurricane, as shown in Moon et al. (2003). However, some detailed wave spectral patterns and spectral factor characteristics around a hurricane's track are smoothed and neglected, due to the inherent limits of numerical models. Observed wave spectra during a hurricane are extremely important in revealing the realistic and detailed spectral properties of hurricane-generated waves.

2.2 *Wind and wave observations*

Figure 1 shows Hurricane Juan's track, Juan's wind swath isolines, and those wind and wave observation stations along Juan's path. Seven buoys within or near the 10 m/s wind swath isoline are selected, as shown in Table 2. From these buoys, sta-

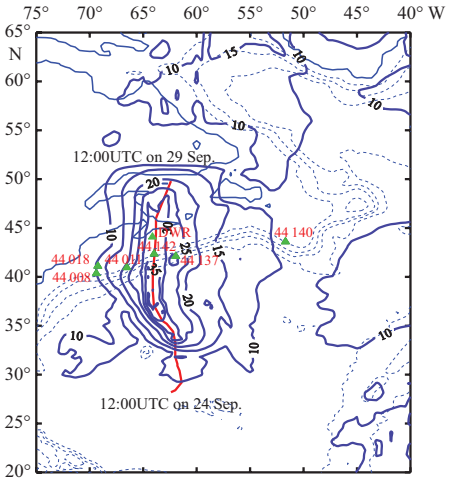

Fig.1. Hurricane Juan's track, wind swath isolines, wind and wave observation stations around Juan's track in the coarse-resolution domain during WW3 simulation.

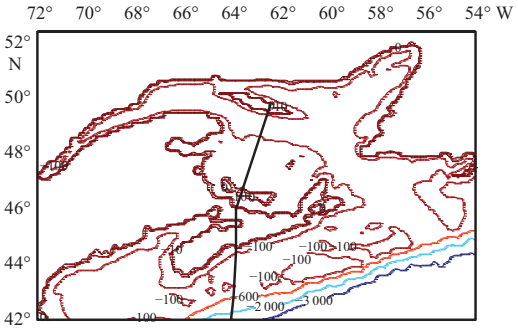

Fig.2. Hurricane Juan's track near the Scotian Shelf in the nesting intermediate-resolution domain.

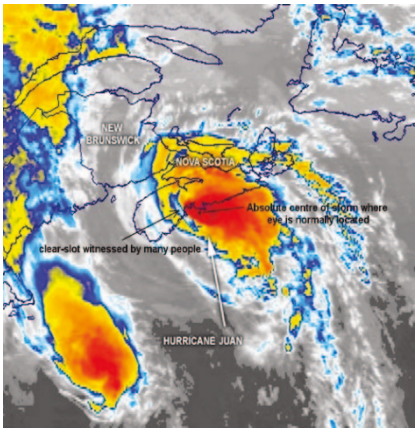

Fig.3. Satellite image when Juan made landfall in Halifax.

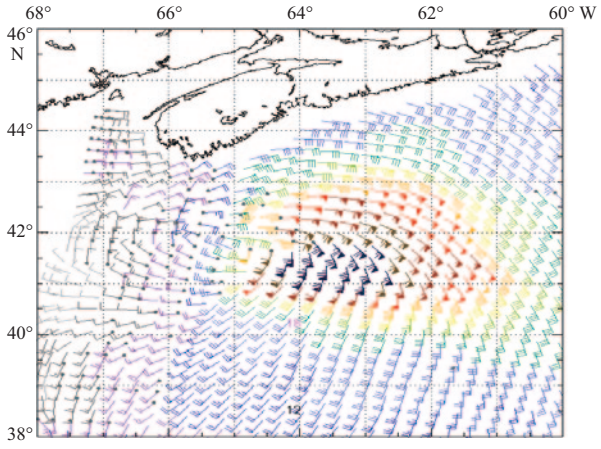

Fig.4. QSCAT winds at 22:12UTC Sep. 28, 2003 when hurricane Juan was near Scotian Shelf.

Table 1. Characteristics and best track of Hurricane Juan

Date (UTC)	Sep. 27	Sep. 27	Sep. 27	Sep. 27	Sep. 28	Sep. 28	Sep. 28	Sep. 28	Sep. 29	Sep. 29
Time (UTC)	03:00	09:00	15:00	21:00	03:00	09:00	15:00	21:00	03:00	09:00
Latitude (N)	33.7°	34.9°	35.3°	35.9°	36.8°	37.6°	39.4°	41.2°	44.5°	47.8°
Longitude (W)	61.9°	62.4°	63.0°	63.4°	63.8°	64.1°	64.1°	64.1°	63.8°	63.4°
MSLP/hPa	984	981	979	970	970	970	973	973	974	987
Eye diameter/km		27.78	27.78	37.04		27.78				
Max. wind /m·s^{-1}	36.01	38.58	38.58	46.30	46.30	46.30	43.72	43.72	36.01	30.86
34 kn NE/rad·km^{-1}	324	324	324	324	324	324	370	370	278	278
34 kn SE/rad·km^{-1}	185	185	185	222	222	222	278	278	185	278
34 kn SW/rad·km^{-1}	93	111	111	111	93	148	185	185	185	185
34 kn NW/rad·km^{-1}	222	222	222	222	222	222	350	222	185	278
50 kn NE/rad·km^{-1}	56	74	74	74	93	93	111	111	111	148
50 kn SE/rad·km^{-1}	56	74	74	74	93	93	111	111	111	148
50 kn SW/rad·km^{-1}	56	74	56	56	93	93	111	111	111	74
50 kn NW/rad·km^{-1}	56	74	74	74	93	93	111	111	111	74
64 kn NE/rad·km^{-1}	37	37	37	46	56	56	111	111	111	
64 kn SE/rad·km^{-1}	37	37	37	46	56	56	56	56	56	
64 kn SW/rad·km^{-1}	37	37	37	46	56	56	56	56	56	
64 kn NW/rad·km^{-1}	37	37	37	46	56	56	56	56	56	

Notes: Mean sea level pressure is denoted as MSLP; kn is the symbol for knot–a unit of speed, nautical miles per hour, 1 kn=1.852 km/h.

tions 44140, 44008, 44018, and 44011 are located in intermediate water depth (from now on, Station is denoted by Sta.), Stas 44142 and 44137 are in deep water. Station 44142 is on the storm track; Sta. 44137 is on the right side of the track, outside of the maximum wind radius; Sta. 44011 is on the left side of the 20 m/s wind swath isoline; Sta. 44140 is on the right side of the 10 m/s wind swath isoline; Stas 44008 and 44018 are on the left side of the 10 m/s wind swath isoline. One-dimensional observed wave spectra are available in these locations. The DWR buoy is near the coast in shallow water: it is exposed to the open ocean. Sta. DWR was about 25 km to the left of Juan's track, so two-dimensional spectra are available at this station during Juan's passing.

Figures 5a and b give observed wind velocities and wind directions at Stas 44142, 44137, and 44258 during Hurricane Juan. Buoy 44137 was about 150 km to the right side of Juan's track. The observed data for this station showed that wind speed increased from 18.4 to 21.4 m/s, then decreased to 19.3 m/s over the time interval from 22:20UTC on Sep. 28 to 00:20UTC on Sep. 29, 2003. Within the same timeframes, the data also revealed that wave heights (H_s) increased from 6.1 to 6.9 m, then decreased to 6.7 m. Buoy 44142 was located on Juan's track, so it recorded wind speed increasing from 20 to 28.1 m/s, then decreasing to 18.7 m/s; correspondingly H_s increased from 8.0 to 12.1 m and then decreased to 9.8 m. However, over the time interval from 22:20UTC on Sep. 28 to 00:20UTC on Sep. 29, at DWR, wind speed increased from 18.4 to 21.4 m/s and then decreased to 19.3 m/s, while H_s increased from 6.8 m to 9.2 m and then went down to 6.7 m, during 03:11–05:11UTC on Sep. 29, 2003. Recorded winds and waves at buoys 44142, 44137, and DWR reflected how different wave properties in different locations related to the passage of Hurricane Juan, as illustrated in Table 3.

Table 2. Observation stations around Juan's track

Station	44137	44142	44008	44018	44011	44140	DWR
Water depth/m	1 300	4 500	62.5	74.4	88.4	90.0	29.0
Location	42.26°N	42.50°N	40.50°N	41.26°N	41.11°N	43.75°N	44.24°N
	62.00°W	64.02°W	69.43°W	69.29°W	66.58°W	51.74°W	64.18°W
Spectral type	1-D	1-D	1-D	1-D	1-D	1-D	2-D

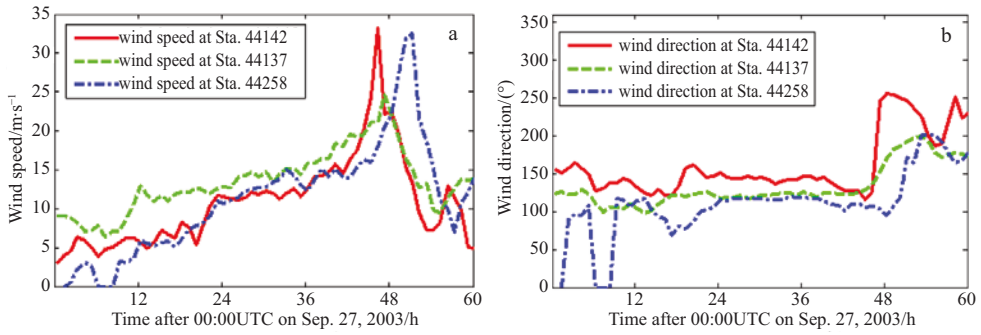

Fig.5. Wind speed and wind direction at Stas 44142, 44137 and 44258 during Hurricane Juan.

Table 3. Observed winds and significant wave heights at buoys 44137, 44142, and DWR during Juan's peak time

Station	Time (hour UTC day)	Wind speed/m·s^{-1}	H_s/m
Buoy 44137	22:20UTC 28	18.4	
	23:20UTC 28	21.4	6.1
	00:20UTC 29	19.3	6.9
	01:20UTC 29		6.7
Buoy 44142	21:20UTC 28	20.0	
	22:00UTC 28	28.1	8.0
	23:20UTC 28	18.7	12.1
	00:20UTC 29		9.8
DWR	03:11UTC 29	20.0	6.8
	03:41UTC 29	17.2	9.2
	05:11UTC 29	12.0	6.7

3 Waves around Juan's track during Hurricane Juan

3.1 *Wave composition analysis based on time series of one-dimensional frequency spectra*

Figure 6 shows the time series of one-dimensional (1-D) frequency spectra measured at buoys 44137, 44140, 44008, 44011, 44142, and 44018. This kind of 1-D spectral pattern is also called Munk-Barber-Ursell diagram (Barber and Ursell, 1948; Snodgrass et al., 1966). With a northward propagation direction from beginning to landfall, and with accelerating translation speed most of the time, the swell components in these Munk-Barber-Ursell diagrams show paroxysmal behaviour at most of these locations (except for Buoy 44140), during the hurricane.

It can be seen that waves at different locations show totally different behaviours in strength, duration, and spectral pattern. In areas along Juan's track and on the left of the track, dominant swell existed almost over 24 hours before, during, and after Juan's passage (Stas 44142, 44137, 44011, 44008, and 44018). Checking Juan's wind swath isoline (Fig. 1), Sta. 44140 is on the right side of the 10 m/s wind swath isoline, so it is very slightly influenced by hurricane-generated waves: both wind sea and swell are very small. Meanwhile, Stas 44008 and 44018 on the left side of 10 m/s wind swath isoline are seriously influenced. At Sta. 44011, dominant swell existed over 24 h. At Sta. 44142, the combination of extremely low frequency strong swell plus

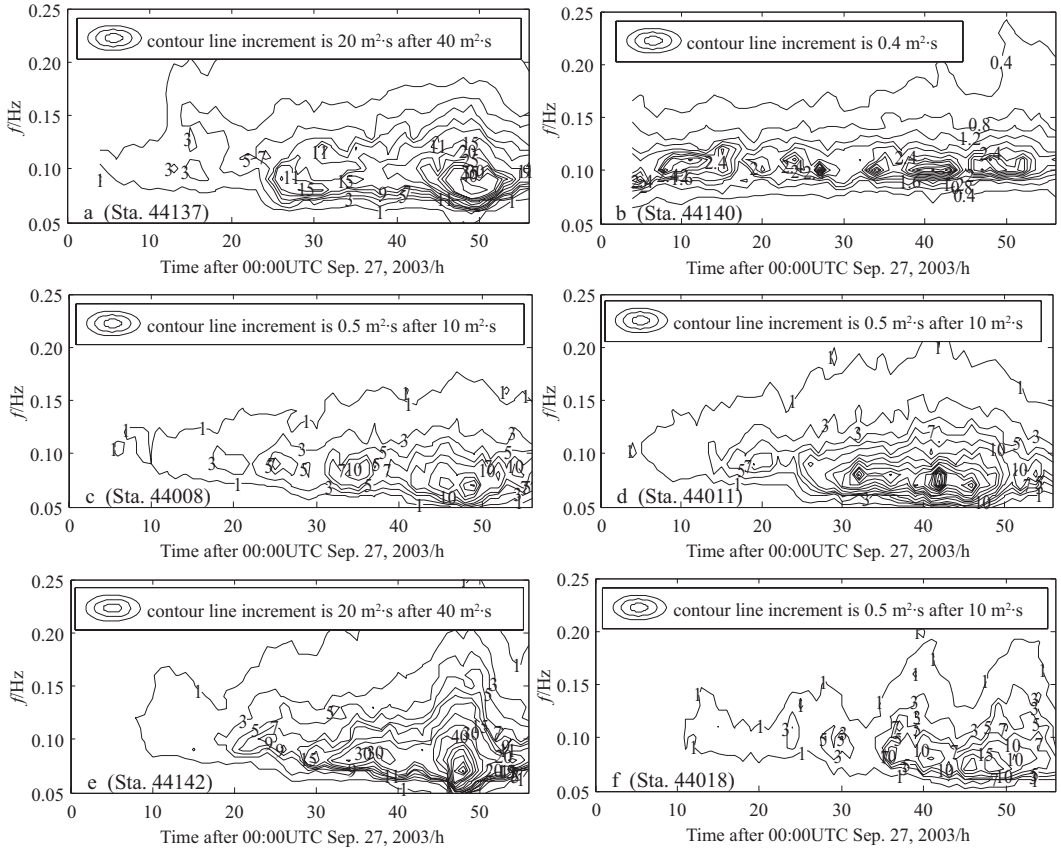

Fig.6. Observed one-dimensional time series frequency spectra around Juan's track at Stas 44137, 44140, 44008, 44011, 44142, and 44018.

the strong wind sea forms a strong spectral sharp peak within short time, with strong hybrid peak waves lasting for about two hours. At Sta. 44137, swell existed over 24 h, with strong peak waves (swell plus wind sea) lasting for about three hours.

Therefore, location is an important factor for hurricane-generated wave spectral composition, strength, and duration. Interestingly, with the same water depth, in the same wind swath isoline, and located along 10 m/s wind swath isoline, the time series of one-dimensional frequency spectra at Stas 44008, 44018, and 44140 show different spectral patterns.

3.2 *Wave steepness during Hurricane Juan*

Wave steepness is defined as the ratio of wave height to length: the National Data Buoy Center (http://www.ndbc.noaa.gov/windsea.shtml) has been using wave steepness to estimate wind seas and swell since 1997, by determining a separation frequency, assuming that wind seas are steeper than swell and that maximum steepness occurs in the wave spectrum near the peak of wind seas energy. In this study, general wave steepness is calculated with $S=\frac{H_s}{L}=\frac{2\pi f_m^2 H_s}{g}$, in which, H_s, L and f_m are significant wave height, wave length, and average wave frequency, respectively. Figure 7 gives wave steepness at Stas 44142, 44137, 44011, 44018, 44008, 44140, and DWR stations during the hurricane.

Figure 7 indicates that wave steepness is higher on the right side of Juan's track (Sta. 44137), lower on the left side (Stas 44011, 44018, 44008, and DWR). Wave steepness reaches the highest value at Juan's peak, decreasing after Juan passes each station. The biggest wave steepness occurs on the track at Juan's peak time (Sta. 44142). Higher wave steepness means more wind wave component, and lower wave steepness means more swell component. Sta. 44140 is near 10 m/s wind swath isoline on the right side of Juan's track, and its wave steepness is almost unchanged during hurricane process; the reason is that Sta. 44140 is almost not influenced by hurricane-generated waves. As indicated in Fig. 6b, Sta. 44008 is on the 10 m/s wind swath isoline to the left side of Juan's track, and its wave steepness is slightly influenced. However, wave steepness at Sta. 44008 is higher than that of Sta. 44140 during the whole hurricane, which implies that this location was affected more than Sta. 44140 during most of Juan's process. Sta. 44018 shows interesting behavior with regular undulation of semidiurnal cycle around the wave steepness curve of Sta. 44008, even though Sta. 44018 is near Sta. 44008, and even though it falls along the 10 m/s wind swath isoline. Sta. 44018 is located in the Great South Channel between Nantucket and Georges Bank, in the Gulf of Maine, as shown in Fig. 8. The Gulf of Maine is home to the highest tidal

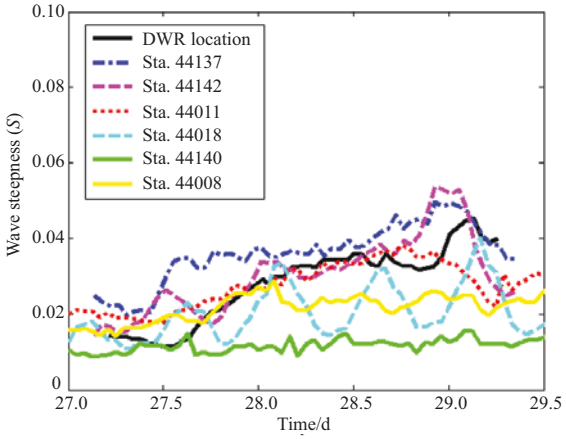

Fig.7. Wave steepness at Stas 44142, 44137, 44011, 44018, 44008, 44140, and DWR during the hurricane.

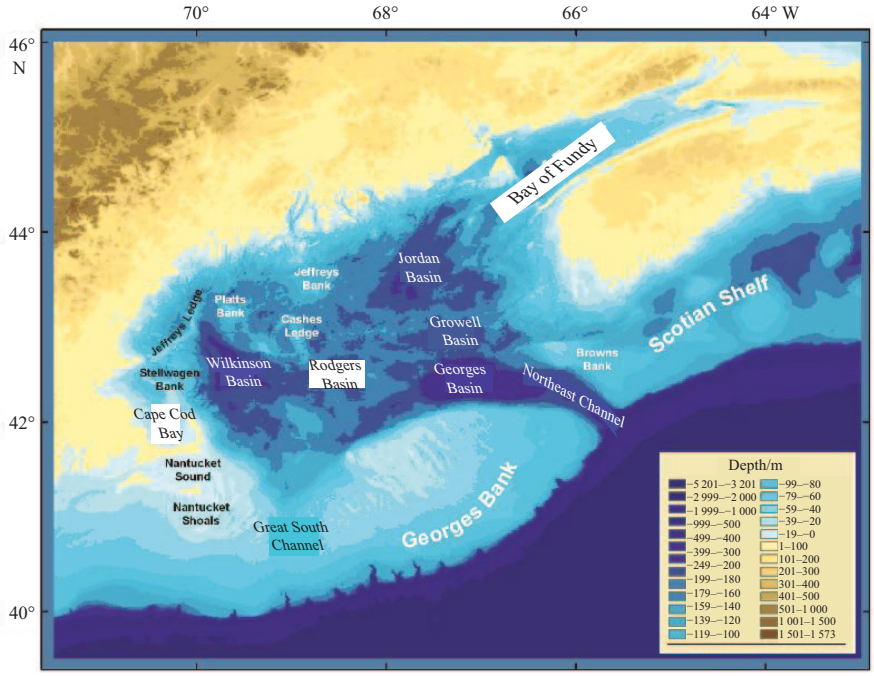

Fig.8. Map of Gulf of Maine, Great South Channel and Sta. 44018.

elevation on the planet, where strong semidiurnal tides flood and ebb through the Great South Channel. Therefore, the strong fluctuations of wave steepness at Sta. 44018 are attributed to the strong wave-current interactions during Hurricane Juan.

4 Wave spectral involvement during Hurricane Juan

4.1 *One-dimensional spectra*

Three stations (44142, 44137, and DWR) are selected in the order that typical spectral variation behavior will be explored in deep and shallow water, on the right side, left side, and on the track of Hurricane Juan. Figures 9, 10, and 11 show the 1-D wave spectra at Stas DWR, 44137, and 44142: before, during, and after Juan's passing. These observed spectra show dramatic changeable spectral pattern, multiple peaks, and swell dominant features during the hurricane process, whether in deep or shallow water.

Observed 1-D wave spectra show that spectral shape changes dramatically during Hurricane Juan, and low frequency swell spectral energy dominates before, during, and after Juan's passing. Spectral peak and spectral energy reaches the highest value during Juan's peak time, at different locations on the track, to the left and right side of the track. Obvious multi-peak spectral shape is observed at these three stations, especially around Juan's peak time, which means that strong swell and strong wind waves coexist during peak time, whether in deep open

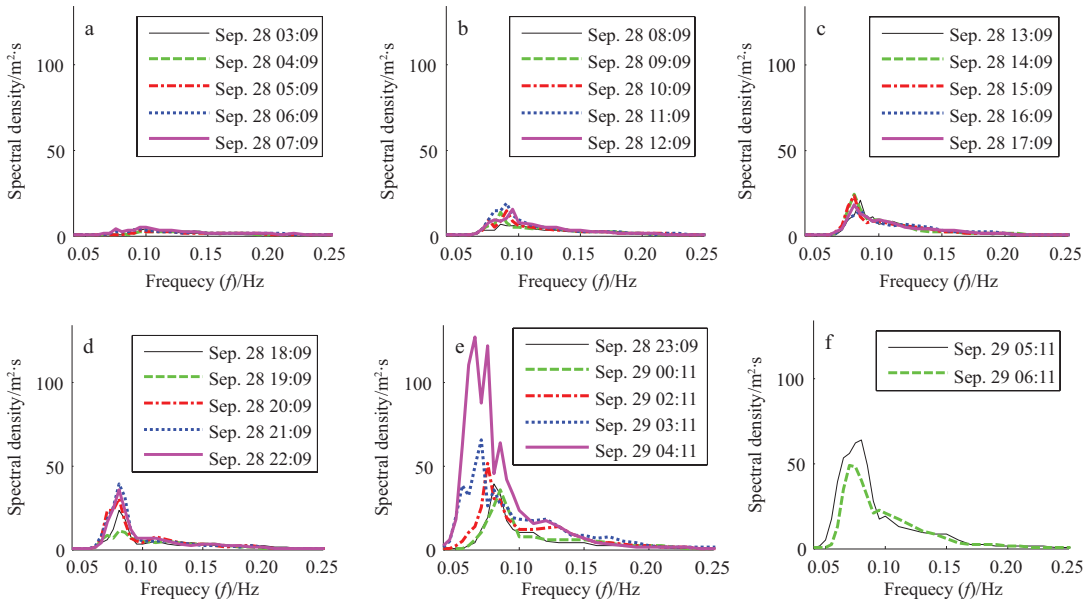

Fig.9. Juan generated 1-D wave spectra at Sta. DWR from Sep. 28 to 29, 2003.

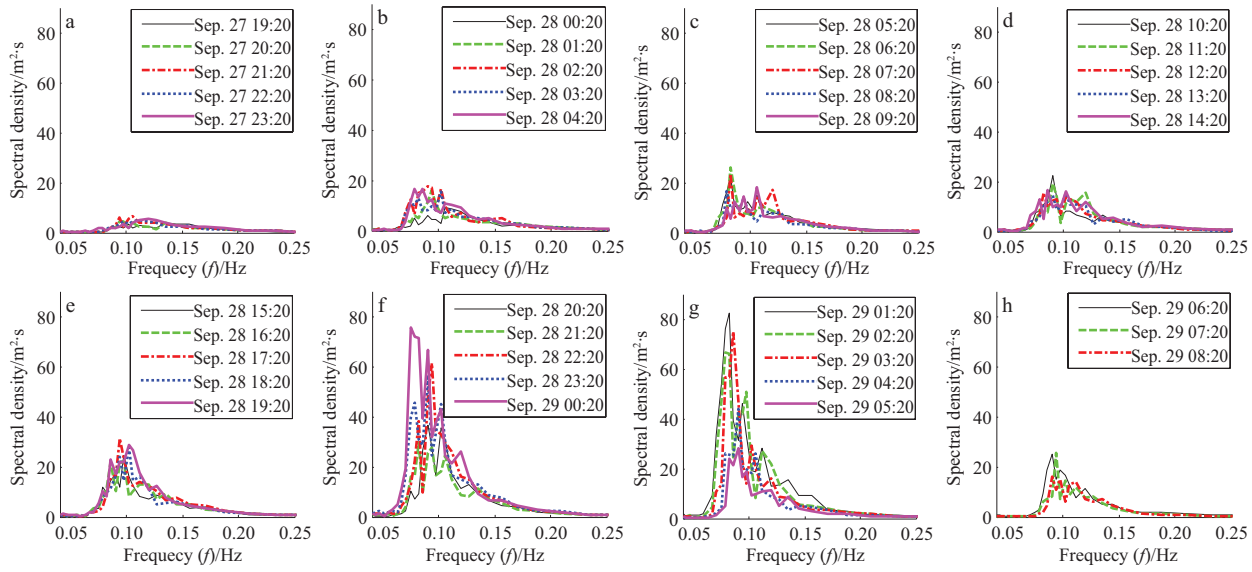

Fig.10. Juan generated 1-D wave spectra at Buoy 44137 from Sep. 27 to 29, 2003.

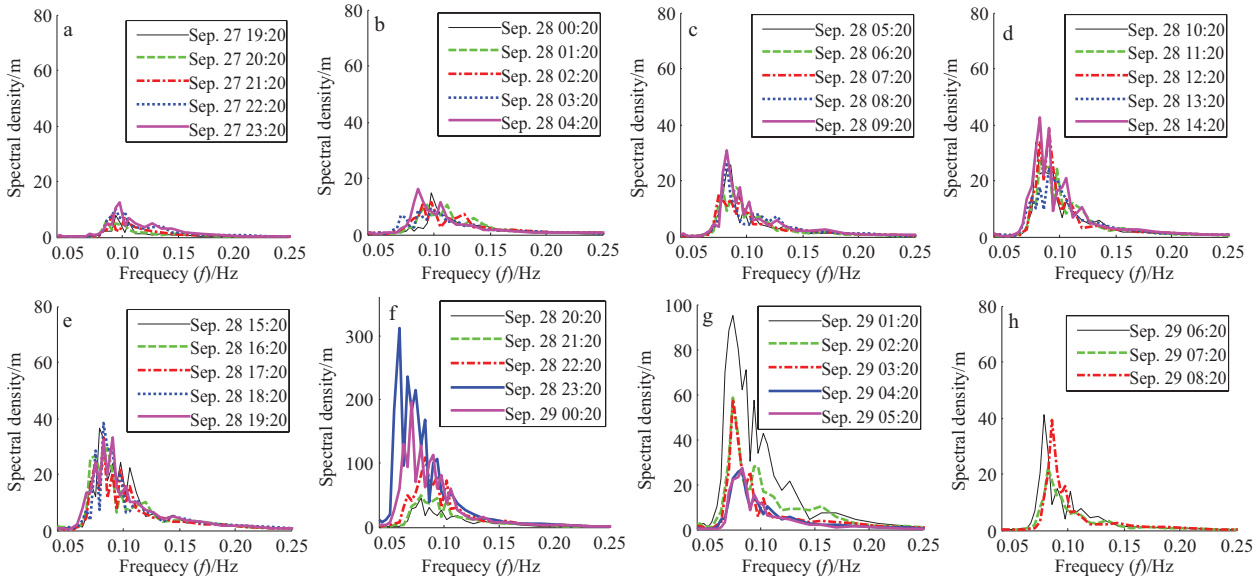

Fig.11. Juan generated 1-D wave spectra at Buoy 44142 during Hurricane Juan process from Sep. 27 to 29, 2003.

ocean, intermediate water depth, or shallow coastal water.

4.2 *Two-dimensional wave spectra at Sta. DWR*

Sta. DWR is located in coastal shallow water. Observed two-dimensional wave spectra in Fig. 12 indicate that dominant wave directions and directional distributions are limited to a specified narrow range during Hurricane Juan. As Juan's wind began to affect Sta. DWR, there was already a rather small spectral density swell component at low frequency. As Juan moved northward, winds at Sta. DWR became stronger, swell spectral density energy increased, maximum spectral density energy remained with rather stable directional distribution (70°–100°) during Juan's course. Sometimes, there were more than three spectral peaks within the two-dimensional spectra. Main wave

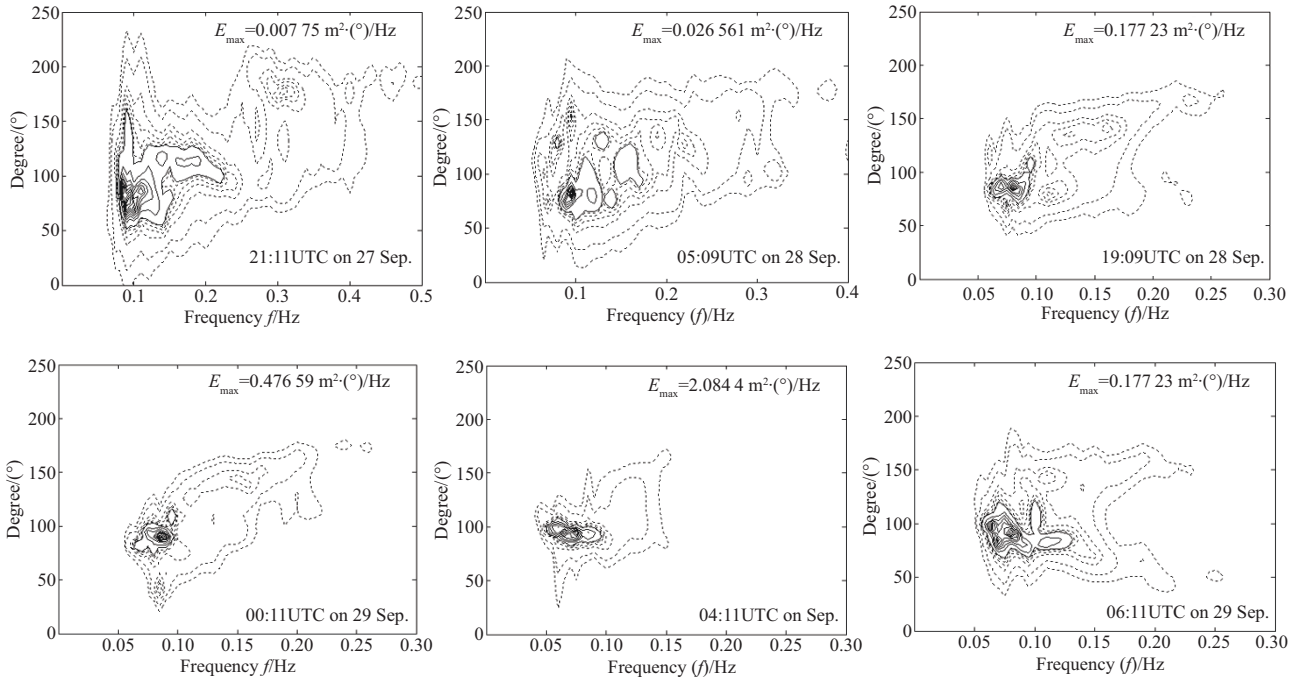

Fig.12. Two-dimensional spectra at Sta. DWR from 21:11UTC on Sep. 27 to 06:11UTC on Sep. 29 2003. All values of E_{max} are divided by 2π. Dashed lines from outer to inner loops are 0.005, 0.01, 0.03, 0.05, 0.07, and 0.09; solid lines are 0.1, 0.2, … , 0.9, and 1, respectively. Wave direction follows Cartesian convention: 0° to the east, in counterclockwise direction.

energy distributes within narrow directional and frequency bands, wind wave spectra superposed on the swell spectra. The maximum spectral density values grow rapidly with the maximum value occurring when Juan passed Sta. DWR. After Juan passed Sta. DWR, the spectral density decreased, and the directional and frequency distributions became wider.

5 Standardization of the observed wave spectra during Hurricane Juan

5.1 *Standardized observed 1-D wave spectra at Stas 44142 and 44137*

Figures 13a and 14a are observed one-dimensional spectra during Hurricane Juan at Stas 44142 and 44137, respectively. Figures 13b and 14b are standardized one-dimensional spectra, $S(f)f_p/E$, in which, $S(f)$, f_p and E are wave frequency spectrum, peak frequency, and wave spectral density, respectively. Figures 13c and 14c are standardized one-dimensional spectra $S(f)f_0/E$, in which, f_0 and E are average frequency and wave energy, respectively. The standardized one-dimensional spectra generally have similar shape, peak, and spectral width, in spite of the dramatic variation during the whole hurricane, as shown in Figs 9, 10, 11, 13a, and 14a. In particular, those standardized by the average frequency in Figs 13c and 14c are more reserved and similar in spectral shape during the whole hurricane. This implies that the main properties of these standardized spectra generally can be expressed in a simple uniform form, and average frequency is more suitable to standardize spectra than peak frequency; the reason will be integrated in Section 5.2.

5.2 *Peak frequency and average frequency during hurricane process*

Among the wave frequency parameters examined herein (spectral peak frequency, average wave frequency), peak frequency is the most commonly used wave parameter, but it shows unstable behavior, as shown in Fig. 15a, due to spectral multi-peak distributions or problems in processing observational data. Average wave frequency is also sensitive to sea state and data processing techniques: the narrower the spectral shape, the smaller the difference between spectral peak frequency and average wave frequency. In addition, average wave frequency is also affected by wave surface sampling interval and recorded frequency resolution.

The zero-crossing average wave frequency can be obtained by $\bar{f} = f_{0,2} = \left(\frac{m_0}{m_2}\right)^{-0.5}$, in which, m_0 and m_2 are defined as $m_0 = \iint S(f,\theta)\mathrm{d}f\mathrm{d}\theta$, $m_2 = f^2 \iint S(f,\theta)\mathrm{d}f\mathrm{d}\theta$. Another average wave frequency $f_{0,1}$ is defined as $f_{0,1} = \left(\frac{m_0}{m_1}\right)^{-1}$, in which, $m_2 = f^2 \iint S(f,\theta)\mathrm{d}f\mathrm{d}\theta$. Compared with $f_{0,1}$, $f_{0,2}$ is affected more

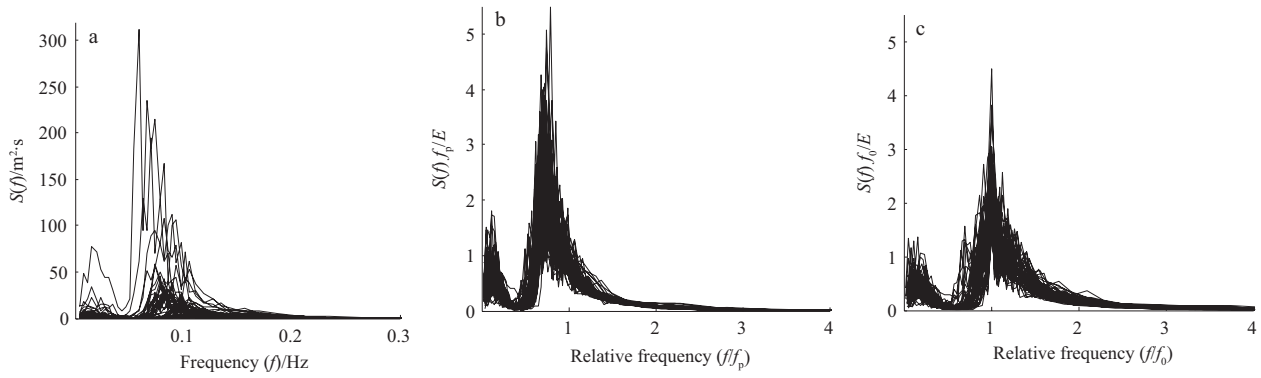

Fig.13. Observed hourly 1D spectra (a), relative 1D spectra standardized by peak frequency (b), and relative 1-D spectra standardized by average frequency (c), at Sta. 44142 from 03:20UTC on Sep. 27 to 08:20UTC on Sep. 29, 2003.

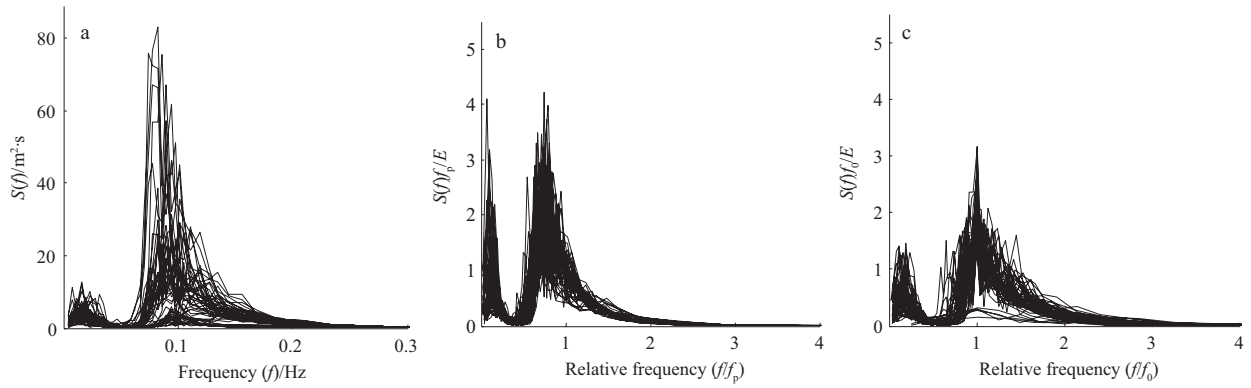

Fig.14. Observed hourly 1-D spectra (a), relative 1-D spectra standardized by peak frequency (b), and relative 1-D spectra standardized by average frequency (c), at Sta. 44137 from 03:20UTC on Sep. 27 to 08:20UTC on Sep. 29, 2003.

by the spectral high frequency tail. At Stas DWR, 44137, and 44142, the correlation coefficient between $f_{0,1}$ and peak frequency f_p are 0.841 3, –0.202 0, and 0.808 9 respectively; the correlation coefficient between the $f_{0,2}$ and f_p are 0.836 9, –0.258 8, and 0.778 5 respectively; thus $f_{0,1}$ is more related with peak frequency, compared with $f_{0,2}$.

Figure 15 gives observed peak frequency f_p, observed average frequency $f_{0,1}$, and observed average frequency $f_{0,2}$ at Stas 44142, 44137, and DWR during the hurricane process. The similar variation tendencies of f_p, $f_{0,1}$, and $f_{0,2}$ throughout Juan's course are shown at the three stations. In these figures, peak frequency f_p shows vehement ups and downs for the three stations, and it is difficult to give a clear interpretation of the variation tendency. Meanwhile, both $f_{0,1}$ and $f_{0,2}$ show more stable variation tendency during Hurricane Juan's development, compared with the observed peak frequency. Before Juan's passing, average frequency at these three stations decreases, reaches the lowest point during peak time, and increases afterwards. It can be seen that different locations around Juan's track show different frequency change patterns: at Sta. DWR, there is the highest average frequency before Juan's passing. That is why average frequency has the ability to provide more uniform standardized spectral shape, compared with peak frequency, as indicated in Figs 13c and 14c.

6 Spectral width variations during hurricane process

Spectral width is defined as $\varepsilon = \left(1 - \frac{m_2^2}{m_0, m_4}\right)^{1/2}$ (Cartwright and Longuet-Higgins, 1956), in which, the fourth-order moment m_4 not only depends on the spectral shape, but also on the high frequency cut-off, errors, and nonlinear disturbances in the high-frequency part of the spectrum. Another spectral width parameter $\xi = \left(m_0 \cdot \frac{m_2}{m_1^2} - 1\right)^{1/2}$ is suggested (Longuet-Higgins, 1975), which is less dependent on high-frequency instability. Both the spectral width parameters satisfy ξ, $\varepsilon \in (0,1)$. Waves can be seen as narrow spectra, when $\xi \to 0$, and $\varepsilon \to 0$. For fully developed PM spectrum (Pierson and Moskowitz, 1964), ξ=0.425, ε=1; for JONSWAP spectrum (Hasselmann et al., 1973), ξ=0.389, ε=1. Therefore, PM and JONSWAP type spectra can be regarded as wide-band spectra. If the spectrum is not narrow, it implies that there are many local water surface ups and downs, and these fluctuations do not cross with average water level, so it cannot be recorded into wave zero-crossing movement.

Figure 16 shows spectral width variations of ξ and ε at Stas DWR, 44142, and 44137, during hurricane Juan. Values of ξ at Stas DWR, 44142, and 44137 are within the range of 0.35 to 0.6; values of ε at Stas DWR, 44142, and 44137 are within the range of 0.65 to 0.83, so hurricane-generated waves are wide-band spectral waves during Juan's course. Interestingly, spectral bands at each station remain stable during the whole hurricane, with the widest band spectra at Sta. DWR, then Sta. 44142; and the narrowest at Sta. 44137. Spectral width becomes wider and wider from the right side, on the track until the left side of Juan's track.

Spectral width at each station changes slightly before, during, and after Juan's passing, even though the real spectral peak

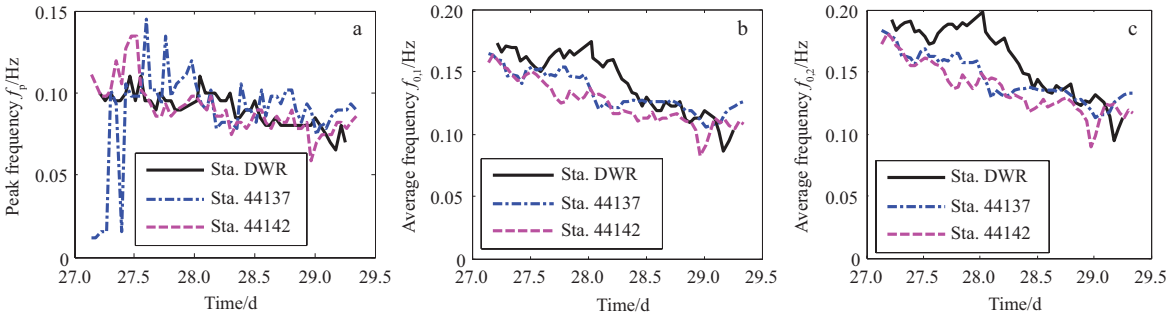

Fig.15. Observed peak frequency (a), observed peak frequency $f_{0,1}$ (b), and observed peak frequency $f_{0,2}$ (c), at Stas 44142, 44137, and DWR from 03:20UTC on Sep. 27 to 08:20UTC on Sep. 29, 2003

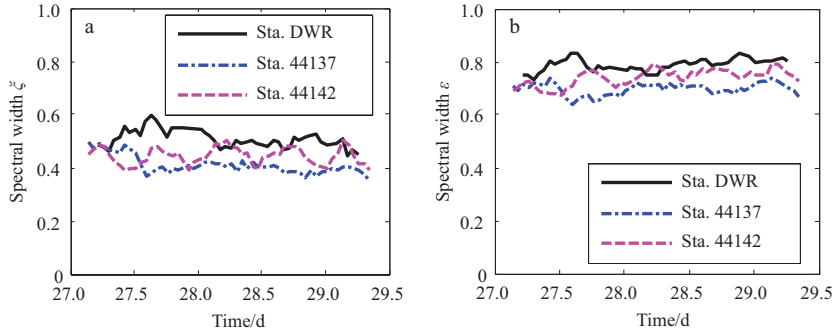

Fig.16. Spectral width values of ξ (a), and ε (b) at Stas DWR, 44142, and 44137 during Juan's course.

frequency, spectral energy, and spectral peak change dramatically during the hurricane as indicated in Figs 9, 10, and 11. This also confirms that a uniformly standardized form can grasp most of the spectral wave characteristics, even with complicated hurricane-generated waves. In the next step, adaptability of JONSWAP spectral form in formulating hurricane-generated wave spectra will be evaluated.

7 Simulated wave spectra during Hurricane Juan

A two-layer nested WW3 (Tolman, 2002) simulation is implemented in this study. Computational domains are chosen according to Hurricane Juan's path, swell propagation characteristics, and the storm's translation speed, in order to optimally simulate the hurricane-generated wave energy. The coarse-resolution domain is from 20° to 65°N and 40° to 75°W, as shown in Fig. 1. An intermediate-resolution domain is nested within this first region, covering most of the waters off eastern Canada and the New England States, bounded by 42° to 52°N and 55° to 71°W, as shown in Fig. 2. Whereas space resolutions are 15′ and 5′, respectively, directional resolution in all domains is 6°. Frequencies range from 0.030 94 to 0.593 90 Hz, with neighboring frequencies defined as f_{n+1} =1.1f_n. An interpolation methodology to blend observations with COAMPS (Coupled Ocean Atmosphere Prediction System) operational forecast winds is developed to ensure accurate model-driven winds (Xu et al., 2007).

Observed 1-D wave spectra were collected at buoys 44137 and 44142, and observed 2-D wave spectra at Sta. DWR. Figures 17 and 18 compare the simulated 1-D spectra with observations at buoys 44137 and 44142. Generally, the simulated 1-D spectra match the observations, over the entire frequency range: before, during, and after the highest winds occurrences, under wind wave-dominated as well as swell-dominated conditions. Figure 19 compares simulated 2-D wave spectra with

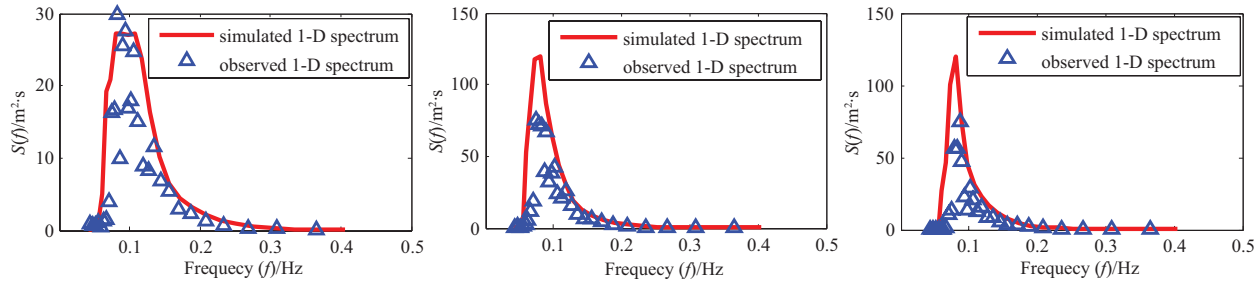

Fig.17. Spectral comparisons of observations with WW3 simulations at buoy 44137.

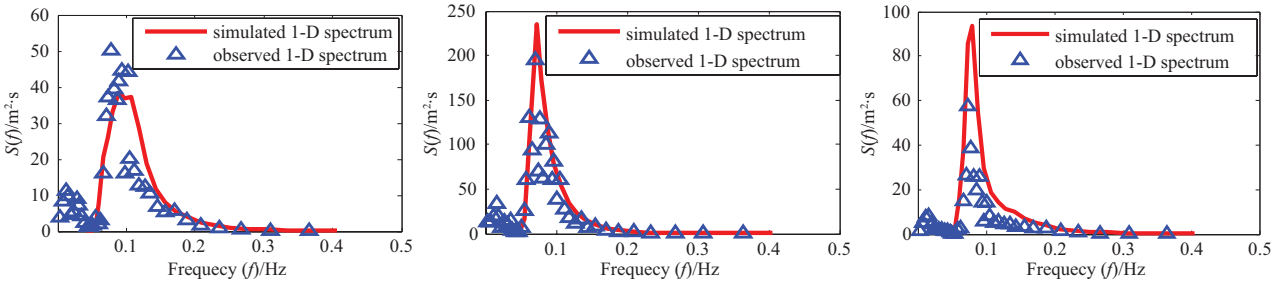

Fig.18. Spectral comparisons of observations with WW3 simulations at buoy 44142.

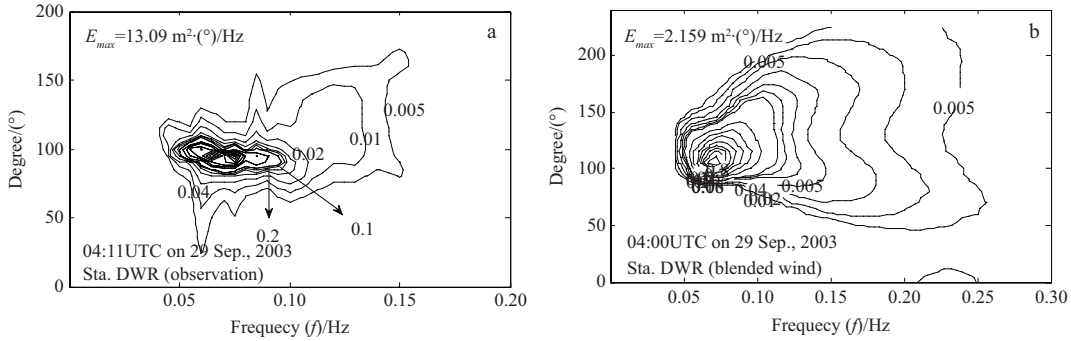

Fig.19. Comparisons of observed (a) and WW3 simulated 2D wave spectra (b) at Sta. DWR, at the time of maximal wave energy; contours indicate fraction of E_{max}. Contours' range values are 0.005, 0.010, 0.020, 0.040, 0.060, 0.080, 0.100, 0.200, 0.300, …, 1.000.

the observations of Sta. DWR at the time of maximum waves. The simulated 2-D spectra do not fit so well with observed 2-D spectra at Sta. DWR, compared with the simulated 1-D spectral validation. While wind-waves dominate before the maximum waves are observed, swell is dominant afterwards; at the time of maximum spectral intensity, the spectra are relatively narrow in directional and frequency ranges. The simulated 2-D spectrum at Sta. DWR has wide directional and frequency range distributions, and does not capture the extent of the narrowing of the observed spectrum. However, the WW3 simulated 2-D spectrum at Sta. DWR still shows their ability in reflecting the spectral frequency peak and peak direction to some extent.

8 Conclusions

Hurricane Juan provides excellent opportunities to reveal the hurricane-generated wave spectral properties, being one of the most damaging storms to hit Nova Scotia, Canada, with wind wave observation Stas 44008, 44018, 44011, DWR, 44142, 44137, and 44140 all located within the 10 m/s wind swath isoline, and distributed to the left side of Juan's track, on the track and to the right side of Juan's track, in deep ocean, intermediate water depth and shallow coastal water.

Time series of one-dimensional frequency spectra measured within the 10 m/s wind swath isoline around Juan's track indicate that waves at different locations show totally different behaviours in strength, duration, and spectral pattern. Dominant swell existed almost over 24 h, before and during Juan's passing on the track, and to the left side of Juan's track. While swell is not the dominant factor to the right side of Juan's track. With higher wave steepness to the right side of Juan's track, observed wave steepness around Juan's track also confirms this conclusion.

Observed 1-D and 2-D wave spectra show that spectral energy, spectral peak, peak frequency, and spectral shape change dramatically during the Hurricane Juan's course, at different locations around the track. Multi-peak spectral shape characteristics are obvious, especially during Juan's peak, whether in deep ocean, intermediate water depth or shallow coastal water.

The standardized 1-D spectra generally have a similar shape, spectral peak, and spectral width, in spite of the dramatic spectral variation during the whole hurricane. Compared with peak frequency, average frequency has the ability to provide more conserved standardized spectral shape. Hurricane-generated waves are wide band spectral waves: spectral width changes slightly before, during, and after Juan's passing at each station. Spectral width experiences a slight increase from the right side to the left side of Juan's track.

The simulated 1-D wave spectra generally agree with observations over the entire frequency range, especially during the highest storm waves, at deep water locations at Stas 44142 and 44137. The simulated 2-D spectra can capture the spectral peak waves to some extent, but still cannot simulate the narrow directional and frequency bands of dominant swell waves at Sta. DWR.

References

Barber N F, Ursell F. 1948. The generation and propagation of ocean waves and swell. I. Wave periods and velocities. Phil Trans R Soc London A, 240(824): 527–560

Battjes J A, Zitman T F, Holthuijsen L H. 1987. A reanalysis of the spectra observed in JONSWAP. J Phys Oceanogr, 17(8): 1288–1295

Bouws E, Günther H, Rosenthal W, et al. 1985. Similarity of the wind wave spectrum in finite depth water: 1. Spectral form. J Geophys Res, 90(C1): 975–986

Cartwright D E, Longuet-Higgins M S. 1956. The statistical distribution of the maxima of a random function. Proc R Soc Lond A, 237(1209): 212–232

Fogarty C T, Greatbatch R J, Ritchie H. 2006. The role of anomalously warm sea surface temperatures on the intensity of Hurricane Juan (2003) during its approach to Nova Scotia. Mon Wea Rev, 134(5): 1484–1504

Goda Y. 1988. Statistical variability of sea state parameters as a function of wave spectrum. Coastal Engineering in Japan, 31(2): 39–52

Hasselmann K, Barnett T P, Bouws E, et al. 1973. Measurements of wind-wave growth and swell decay during the Joint North Sea Wave Project (JONSWAP). Dtsch Hydrogr Z Suppl, A8(12): 95

Longuet-Higgins M S. 1975. On the joint distribution of the periods and amplitudes of sea waves. J Geophys Res, 80(18): 2688–2693

Miller H C, Vincent C L. 1990. FRF spectrum: TMA with Kitaigorodskii's f^{-4} scaling. J Waterway, Port, Coastal and Ocean Engineering, 116(1): 57–78

Moon I J, Ginis I, Hara T, et al. 2003. Numerical simulation of sea surface directional wave spectra under hurricane wind forcing. J Phys Oceanogr, 33(8): 1680–1705

Pierson W J Jr, Moskowitz L. 1964. A proposed spectral form for fully developed wind seas based on the similarity theory of S. A. Kitaigorodskii. J Geophys Res, 69(24): 5181–5190

Resio D T, Phil J H, Tracy B A, et al. 2001. Nonlinear energy fluxes and the finite depth equilibrium range in wave spectra. J Geophys Res, 106(C4): 6985–7000

Snodgrass F E, Groves G W, Hasselmann K F, et al. 1966. Propagation of ocean swell across the Pacific. Phil Trans R Soc Lond A, 259(1103): 431–497

Tolman H L. 2002. User manual and system documentation of WAVEWATCH-III version 2. 22. NOAA / NWS / NCEP/MMAB Technical Note 222, 133, http://polar.ncep.noaa.gov/waves/wavewatch/wavewatch.shtml

Xu Fumin, Perrie W, Toulany B, et al. 2007. Wind-generated waves in Hurricane Juan. Ocean Modelling, 16(3–4): 188–205